Miktoarm Block Copolymer Formation via Ionic Interactions

S. Pispas,[§] G. Floudas,*[,†,‡] T. Pakula,[||] G. Lieser,[||] S. Sakellariou,[§] and N. Hadjichristidis*[,§]

Department of Physics, University of Ioannina, P.O. Box 1186, 451 10 Ioannina, Greece, and Foundation for Research and Technology-Hellas, Biomedical Research Institute (FORTH−BRI), Ioannina, Greece, Department of Chemistry, University of Athens, Zografou 15771, Athens, Greece, and Max-Planck Institut für Polymerforschung, Postfach 3148, 55021 Mainz, Germany

Received September 30, 2002; Revised Manuscript Received December 6, 2002

ABSTRACT: Blends of functionalized polystyrenes (3NPS) having three dimethylamino groups {$N(CH_3)_2$} at one end, with sulfonic acid end-capped polyisoprenes (HO_3SPI) were prepared in a ratio of $N(CH_3)_2/SO_3H = 1$. The morphology of these blends was studied by small-angle X-ray scattering and transmission electron microscopy and the associated dynamics by rheology. The results of the microdomain investigation, as well as of the associated dynamics, provide unambiguous evidence for controlled miktoarm star block copolymer formation via ionic interactions.

1. Introduction

Polymer blends tend to phase separate on length scales of micrometer to millimeter sizes, i.e., macrophase separate on length scales much longer than the size of the polymers involved. Block copolymers, on the other hand, show increased miscibility due to the covalent bond which restricts the phase separation to much smaller scales, typically of the size of the polymeric chains involved. These differences are reflected in the values of the product of the overall degree of polymerization N with the interaction parameter χ, (χN) being much higher (higher compatibility) in the diblock copolymer (A−B) case as opposed to the blend (A/B) case ($(\chi N)_{A-B} \gg (\chi N)_{A/B}$). Another method of increasing blend compatibility is by incorporating specifically interacting groups (usually ionic) in the homopolymers forming the blend. The ionic groups, being more polar than the hydrocarbon chains, give rise to an electrostatic driving force for association which exceeds the strong enthalpic interactions of the hydrocarbon chains and results in the formation of block copolymers through ion pairs.

This alternative approach to copolymer formation has been explored in the past in immiscible polymers modified by ionic interactions via a proton transfer from the organic acid end groups of one polymer to the tertiary amine groups of a second polymer.[1,2] Infrared studies, combined with optical microscopy and differential scanning calorimetry, provided some evidence that such mixtures form block copolymers. However, the decisive experimental proof came through the scattering experiments on the relevant length scale, i.e., small-angle X-ray scattering (SAXS).[3] It was shown that the morphology obtained in mixtures of telechelic polymers, end-capped with tertiary amine functionalities, with telechelic polymers terminated with either carboxylic or sulfonic acid end groups, closely resembles that seen in covalent bonded block copolymers. The peak in the SAXS structure factor, with the domain spacing expected from a block copolymer, was the clear proof of the final morphology. Furthermore, the sulfonic acid groups were found to form stronger ionic associations with the tertiary amino groups than the carboxylate moieties. The same study[3] has also shown that the width of the interface remained sharp in these effective copolymers as the order-to-disorder transition was approached. These studies revealed that it is actually feasible to compatibilize immiscible polymer blends via ionic interactions down to the size of the polymer chain.

We mention here parenthetically that the effect of ionic interactions in the self-compatibility of block copolymers is also very strong.[4−6] The tandem interactions present in functionalized block copolymers with ionic groups give rise to multiple levels of organization within the same material. Experiments demonstrated that ionic interactions provide a unique possibility of altering the block copolymer phase behavior. Depending on the position of the functional group with respect to the chain-ends one can enhance or reduce the miscibility of the blocks.[4−6]

In the present investigation we have explored the possibility of formation of complex block copolymer architectures from A/B blends via ionic interactions, i.e., the formation of block miktoarm copolymers of the A_nB type. For this purpose, we mixed polystyrenes having three dimethylamine groups at one end with sulfonic acid terminated polyisoprenes in appropriate proportions to keep the $N(CH_3)_2$:SO_3H ratio equal to 1. We have employed SAXS and transmission electron microscopy (TEM) to obtain the morphology at the relevant length scale as well as rheology to associate the morphological evidence with the viscoelastic response. The present findings give unambiguous evidence for well-controlled miktoarm star block copolymer formation via ionic interactions.

2. Experimental Section

Polymer Synthesis. The polymers used in this study were synthesized by anionic polymerization high vacuum techniques.[7] The synthesis of the polystyrene (PS) samples having three dimethylamino groups was accomplished in a manner similar to the one used for the synthesis of AB_3 miktoarm stars.[8] Briefly, a living PS chain was reacted with a large excess of $SiCl_4$ in order to produce a PS having three reactive Cl atoms at one chain end. The excess of $SiCl_4$ was removed

[†] University of Ioannina.
[‡] Foundation for Research and Technology-Hellas, Biomedical Research Institute (FORTH−BRI).
[§] University of Athens.
[||] Max-Planck Institut für Polymerforschung.

10.1021/ma0256993 CCC: $25.00
Published on Web 01/17/2003

Table 1. Molecular Characteristics of the Samples Employed

sample[d]	M_w[a] (g/mol)	M_n[b] (g/mol)	M_w/M_n[c]
3NPS25K	26 000	24 800	1.04
3NPS65K	67 000	65 000	1.03
HO_3SPI7K	6700[c]	6500[c]	1.04
HO_3SPI20K	21 000[c]	20 600[c]	1.04

[a] By LALLS in THF at 25 °C. [b] By membrane osmometry in toluene at 37 °C. [c] By SEC in THF at 30 °C. [d] The three blends were as follows: blend A, 3NPS25K/HO_3SPI7K ($w_{PS}^{blend} = 0.56$); blend B, 3NPS25K/HO_3SPI20K ($w_{PS}^{blend} = 0.29$); and blend C, 3NPS65K/HO_3SPI7K ($w_{PS}^{blend} = 0.77$).

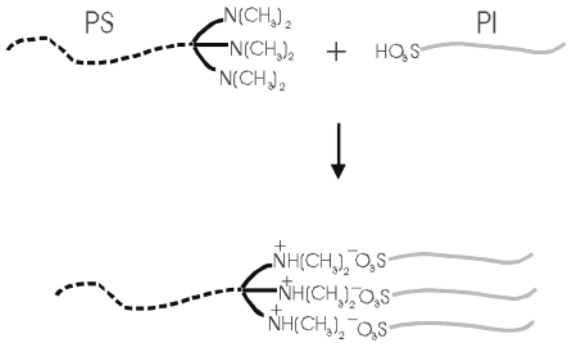

Figure 1. Schematic representation of the formation of a PS−$(PI)_3$ miktoarm star from the PS/PI blend.

on the vacuum line. The PS−$SiCl_3$ macromolecular linking agent was reacted with an excess of a living polybutadiene (PB) oligomer (M_n = 500 g/mol) having a dimethylamine terminal group {$(CH_3)_2$N−PBLi}. This polymer was synthesized by anionic oligomerization of butadiene with the functional initiator (3-dimethylamino)propyllithium.[9] Complete substitution of the chlorines of PS−$SiCl_3$ by the $(CH_3)_2$N−PB resulted in the PS having three dimethylamine groups at one end.

The sulfonic acid terminated polyisoprenes (HO_3SPI) were synthesized according to literature procedures.[10] Isoprene was polymerized using *sec*-BuLi as the initiator; the produced living PILi was end capped with DPE and subsequently reacted with 1,3-propane sultone. The lithium sulfonate group was transformed to the acid form by precipitating the polymer in methanol (containing 20 equiv of perchloric with respect to end groups) three times.[11] The polymers were precipitated once more in pure methanol and dried under vacuum until constant weight.

All samples were thoroughly characterized by a variety of techniques including size exclusion chromatography (SEC), low-angle laser light scattering (LALLS), membrane osmometry, and ^{1}H NMR spectroscopy in terms of molecular weight, molecular weight distribution, and functionality. Their molecular characteristics are given in Table 1.

Blend Preparation. For the preparation of blends, dimethylamine-terminated PS and sulfonic acid terminated PI were dissolved separately in THF. Concentrations of the initial solutions were around 2% w/v in polymer. After complete dissolution of the polymer, the solutions were mixed in the appropriate proportions keeping the $N(CH_3)_2$:SO_3H ratio equal to 1 in all cases. The mixed solutions were transferred in a beaker and the solvent was allowed to evaporate slowly within a period of 5−7 days. Three blends were prepared using the polymers of Table 1. Blend A was formed by mixing 3NPS25K with HO_3SPI7K (3NPS25K/ HO_3SPI7K) ($w_{PS} = 0.56$), blend B by mixing 3NPS25K with HO_3SPI20K (3NPS25K/HO_3SPI20K) ($w_{PS} = 0.29$), and blend C by mixing 3NPS65K with HO_3SPI7K (3NPS65K/HO_3SPI7K) (w_{PS} = 0.77). The blends were then thoroughly dried in a vacuum oven for a period of 1 week. Figure 1 gives a schematic representation of the formation of the miktoarm star copolymers via ionic interactions.

Differential Scanning Calorimetry (DSC). A Mettler Toledo star system was employed capable of programmed cyclic temperature runs. The two samples were first cooled to 123 K at 10 K/min and subsequently heated to 433 K at 10 K/min (first heating). The glass temperatures were obtained from a second cooling/heating cycle between the same temperatures and with the same heating rate. Two glass temperatures were found in all blends. In blend A (3NPS25K/SPI7K), a transition corresponding to PI ($T_g^{PI} = 212$ K with heat capacity Δc_p = 0.29 J/gK) and a much broader transition for PS ($T_g^{PS} = 336$ K) were determined. In blend B (3NPS25K/SPI20K), the corresponding temperatures were: $T_g^{PI} = 219$ K (with Δc_p = 0.35 J/gK) and a much broader transition at $T_g^{PS} = 346$ K. In blend C (3NPS65K/HO_3SPI7K), the two glass temperatures were at $T_g^{PI} = 208$ K and $T_g^{PS} = 350$ K. The broad PS glass temperature range is the norm in block copolymers in contrast to the blend case where the transition range is similar to the corresponding homopolymers.

Rheology. An advanced rheometric expansion system (ARES) equipped with a force-rebalanced transducer was used in the oscillatory mode. Depending on the sample and T range we have made use of two transducers with 2000 and 2 g·cm or 200 and 0.2 g·cm upper and lower sensitivities, respectively. The samples were prepared on the lower plate of the 8 mm diameter parallel plate geometry setup and were heated under a nitrogen atmosphere until flow. Subsequently, the upper plate was brought into contact, the gap thickness was adjusted to 1 mm and the sample was slowly cooled to the desired starting temperature. The elastic (G') and loss (G'') moduli were monitored in different types of experiments. First, the linear and nonlinear viscoelastic ranges were identified, by recording the strain amplitude dependence of the complex shear modulus $|G^*|$. In all subsequent experiments strain amplitudes within the linear viscoelastic range were used (typically below 2%). These experiments involved: (i) isochronal temperature scans within the range 213−403 K (heating and cooling) and (ii) isothermal frequency scans for temperatures in the range 213−403 K and for frequencies $10^{-2} < \omega < 10^2$ rad/s with a strain amplitude of about 2%.

Small-Angle X-ray Scattering (SAXS). An 18 kW rotating anode X-ray source (Rigaku) was used with a pinhole collimation and a two-dimensional detector (Siemens) with 1024 × 1024 pixels. Measurements of 30 min long were made at intervals of 5 K on heating and subsequent cooling within the range 298−553 K, with stability better than ±0.2 K using an appropriate computer program.

Transmission Electron Microscopy (TEM). A LEO EM 912 transmission electron microscope with integrated electron energy-loss spectrometer, operated at 120 kV, was used. Prior to sectioning the blends were exposed in bulk to OsO_4 vapor. Ultrathin sections were produced at about −30 °C using a Leica Low-Temperature sectioning System EMFCS. Micrographs were recorded on Ilford PAN F 35 mm film.

3. Results and Discussion

The existence of a broad polystyrene glass temperature in the DSC traces for the blends provides some hint toward a possible locally varying morphology in the present system as compared to usual PI/PS blends. However, from DSC alone, it is not possible to get direct structural information; therefore, we have employed X-ray scattering, transmission electron microscopy and rheology to unravel the microphase structure and the associated dynamics.

The results from rheology on blend A are summarized in Figures 2 and 3. They are typical also for the other blends B and C. The result of the isochronal run for the storage and loss moduli, shown in Figure 2, depicts different processes which are numbered consecutively starting from lower temperatures and correspond to: (1) the PI glass transition, (2) the spectrum of PI Rouse modes, (3) the PS glass transition, which is followed by a region (4) corresponding to the PS spectrum of Rouse modes and by a region (5) with a parallel behavior of

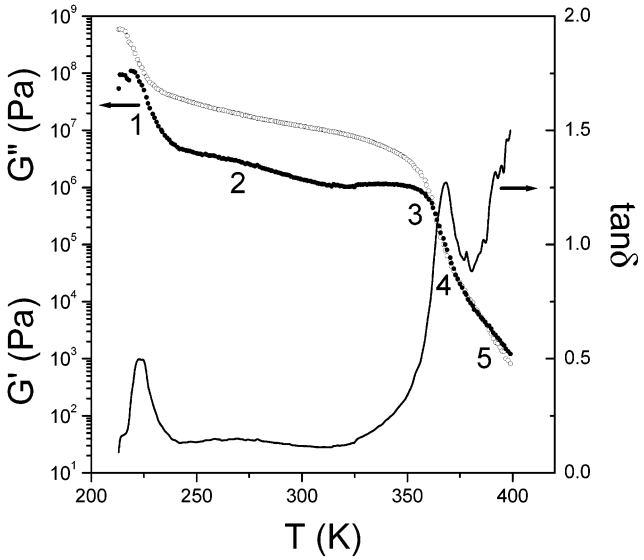

Figure 2. Temperature dependence of the storage (open symbols) and loss (filled symbols) moduli for blend A obtained at a frequency of 1 rad/s with a heating rate of 2 K/min. The loss tangent (tan δ) is also shown with a line. The numbers correspond to the different dynamic regimes (see text).

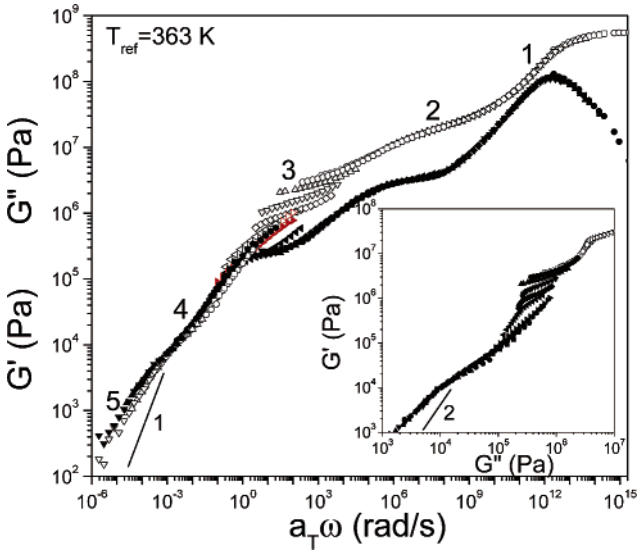

Figure 3. Reduced frequency plots for the storage (open symbols) and loss (filled symbols) moduli of blend A shown at different temperatures. The reference temperature was 363 K, and the strain was below 5%. A line with a limiting slope of 1 is shown at low frequencies. In the inset the data are plotted in the $G' - G''$ representation and exhibit a low-frequency slope which is below 2. Again the numbers indicate the different dynamic regimes.

the moduli where the system does not flow, despite the relatively low molecular weight of the PS/PI blend. This isochronal temperature scan for the "blend" is typical of microphase separated block copolymers and region 5 corresponds to the existence of a microstructure which inhibits the system from flow up to high temperatures. This region is better identified in the frequency dependence (see below) and originates from the slow relaxation of grains. Therefore, Figure 2 constitutes the first proof of microstructure formation in the blends.

The existence of a microstructure results in the breakdown of the time−temperature superposition (tTs) principle since the different processes show distinctly different temperature dependence. Such breakdown is demonstrated by the attempted master-curve construction for blend A in Figure 3. Starting from higher frequencies, the "master-curve" displays the local segmental dynamics (indicated by 1) associated with the PI glass transition, the broad spectrum of PI Rouse modes (2), and the PS glass transition (3) followed by the spectrum of PS Rouse modes (4) and, at lower frequencies, the nearly parallel dependence of the elastic and loss moduli (5) with a slope of about $^1/_2$, which is the fingerprint of the microstructure formation. We should mention here that such parallel dependence of the moduli has been obtained in experiments[12,13] and predicted in theoretical studies[14,15] of lamella-forming block copolymers. Immiscible polymer blends exhibit also thermorheological complexity as a result of the different temperature dependence of the components local friction. However, the observation of $G' \sim G''$ at low frequencies and the inability of the system to flow, despite the low molecular weight and the high temperatures employed (T up to 403 K), suggest the formation of a block copolymer structure in the blends. In Figure 3, we also show the result of the logG' vs log G'' plot (known as the Han representation[16]) which does not rely on any shift, thus providing a direct information on the microstructure formation.

These findings from rheology, which suggest the formation of microdomain morphology in the blends, have direct structural support. In Figure 4, we compare the SAXS profiles of blends A and B at $T = 433$ K. Both profiles show clearly the existence of a peak at low scattering wave vectors (**q**) corresponding to distances of 31 and 47 nm for blends A and B, respectively. Furthermore, the profiles exhibit higher order peaks with relative peak positions at 1:2:3 for blend A, indicating the formation of a lamellar microdomain morphology. There is also an upturn of the intensity at low q's which will be discussed below with respect to the TEM results. For blend B, these features are very broad but the position of the arrows in the figure (relative positions at $1:3^{1/2}:4^{1/2}:7^{1/2}$) could suggest the formation of hexagonally packed cylinders. For blend C, the structure factor maximum is shifted to very low q due to the higher molecular weights involved.

Contrast this situation in the present system with the usual polymer blend case; the structure factor maximum at $q = 0$ in the latter has shifted to finite q values in the former, suggesting that ionic interactions force the system toward increasing compatibility. Furthermore, the ionic interactions are very strong inhibiting access to the disordered state since the order-to-disorder transition temperature is not accessible even by heating the systems to 453 K (in SAXS) i.e., close to the decomposition temperature. This suggests that ionic associations are irreversible.

From the rheology data alone is not possible to access the complete microdomain morphology, i.e., to distinguish between a PI−PS diblock and a specific $(PI)_n$−PS miktoarm star. To account for the microdoamin morphology we use the "phase diagram" proposed by Milner for A_nB miktoarm copolymers.[17] In his approach, the free energies of four phases were considered (lamellar, hexagonal, bicontinuous double diamond, and spherical), and the crossings of these free energy curves determined the phase diagram as a function of volume fraction φ_B and the asymmetry parameter ϵ. The latter was defined as $\epsilon = (n_A/n_B)(l_A/l_B)^{1/2}$, where n_A and n_B are the number of A and B arms, respectively and $l_i = V_i/$

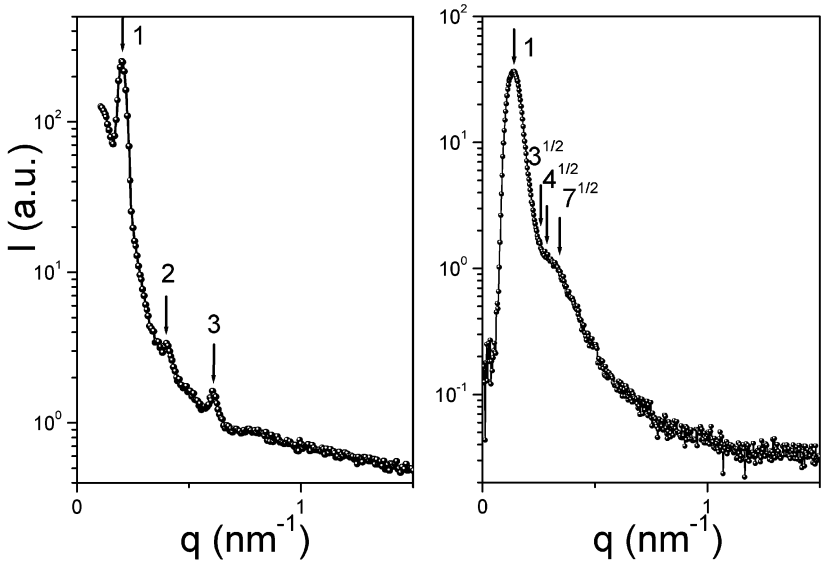

Figure 4. Representative SAXS profiles from blend A (left) and blend B (right) at 433 K. Peaks with relative positions 1:2:3 reveal the formation of a lamellar morphology for blend A. For blend B, an unambiguous assignment of the microdomain morphology is not possible; however, the arrows shown indicate the positions of the main and of some higher order reflections expected from a cylindrical morphology.

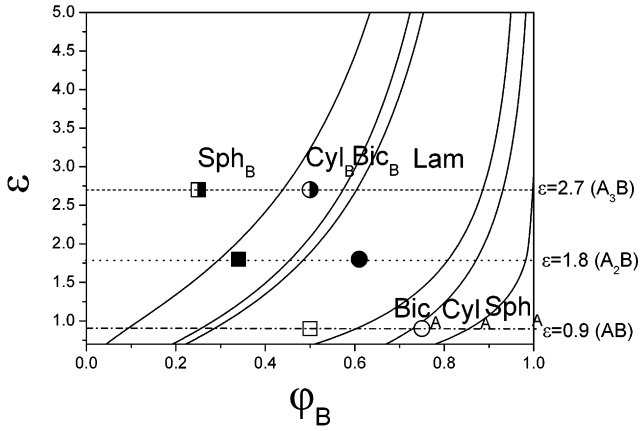

Figure 5. Phase diagram in the strong-segregation limit for A_nB miktoarm star copolymers. The lines are Milner's theoretical predictions. Circles correspond to blend A case and squares to the blend B case. Open symbols indicate the hypothetical formation of an AB diblock, filled symbols the A_2B miktoarm case and half-filled symbols the A_3B miktoarm case. Notice, the good agreement of the A_2B miktoarm case (filled symbols) with the SAXS results for both blends.

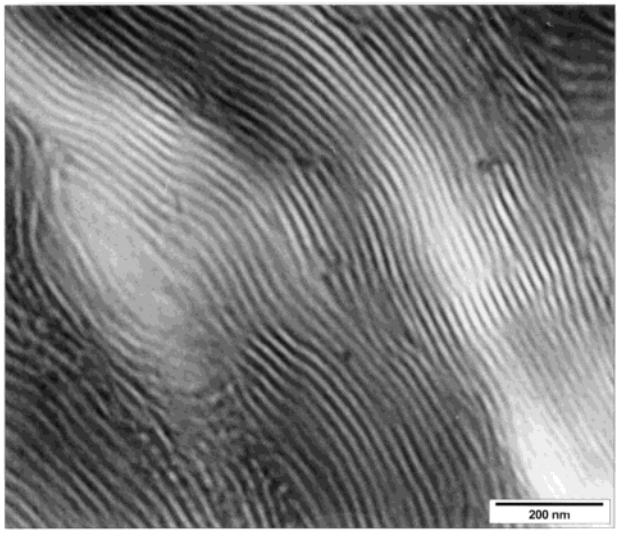

Figure 6. TEM image of blend A from a section stained with OsO_4, revealing a lamellar microdomain morphology.

R_i^2 where V_i and R_i are the molecular volume and radius of gyration of the respective blocks. This approach takes into account chain packing and elasticity effects by treating the miktoarm star layers as brushes having twice as many chains per unit area in the A brush as in the B brush. By construction, this approach is applicable to strongly segregated copolymers, nevertheless, considerable qualitative agreement is found even for weakly segregated miktoarm stars of the A_2B and A_3B type.

The comparison of the present system (blends A and B) with the theoretical predictions is shown in Figure 5. Notice that among the three possible cases, A−B, A_2B, and A_3B, it is the A_2B structure that agrees with the SAXS microdomain morphology in both blends. An A_3B miktoarm would form cylinders and spheres for blends A and B, respectively. This suggests that steric hindrance prevents all three HO_3SPI blocks from association with the 3NPS. The residual PI homopolymer could explain the upturn of the SAXS intensities at low q. Therefore, the SAXS data reveal not only the formation of an A−B block copolymer through ionic interactions but also the formation of a block copolymer with a specific architecture; a miktoarm star copolymer.

TEM provides a direct access to the microdomain morphology through the staining of the PI phase that appears dark. Figure 6 gives the TEM image from blend A and depicts unambiguously a lamellar morphology. Because the lamellar domains in the sample are oriented in various orientations with respect to the direction of sectioning, the distance of the stripes in the micrograph varies according to the tilting of the lamella surface with respect to the knife path. This can explain apparent repeating distances larger than the period corresponding to the SAXS reflection. For lamellar systems in particular, smaller lamellar distances as obtained by SAXS can also be measured in electron micrographs. When one of the components (here PI) has its glass transition below room temperature this component expands after sectioning in thickness giving

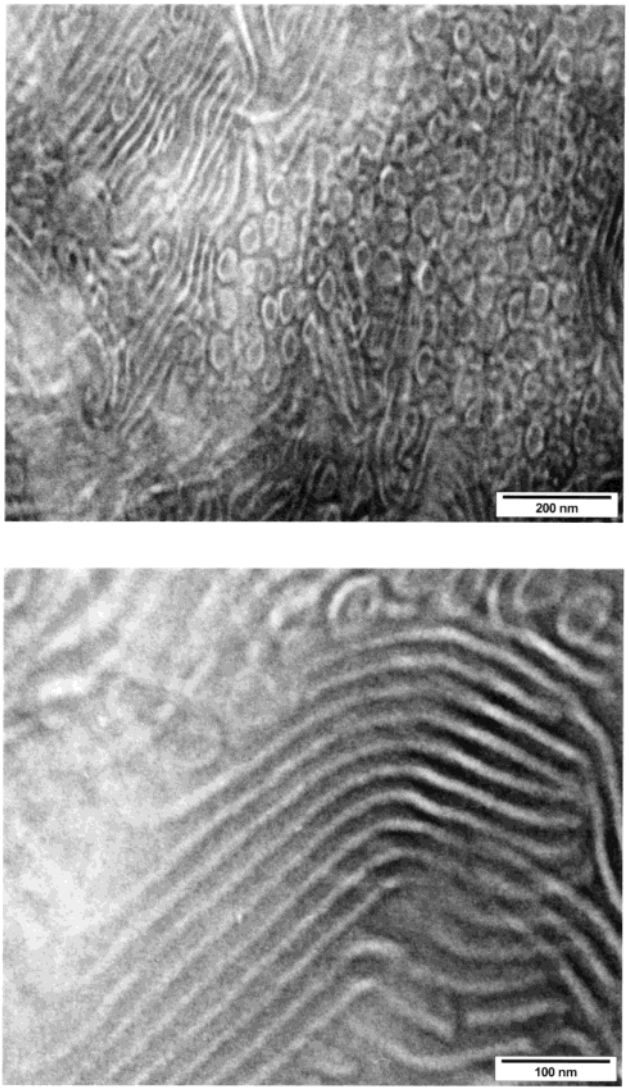

Figure 7. TEM images of blend A from different sections stained with OsO_4. Top: Image of the globular particles of the core−shell type. Bottom: Image of coexisting globular particles with the lamellar morphology.

simultaneously the section rise to shrink laterally.[18] Under this premise the characteristic lamellar spacing of about 25 nm measured on the micrograph agrees reasonably well with the one obtained from SAXS.

Apart from the identification of the predominant lamellar morphology, TEM also provides evidence for some circular moieties that cannot be described unambiguously: their overall size varies supporting a picture of globular particles of the core−shell type with PI as the core. One has to consider that the thickness of a section is roughly between 30 and 50 nm. When globular particles of similar size are sectioned, the diameter of the cross sections gives only an apparent value of the globule diameter. At present, we cannot exclude curved lamellae without long-range order. The origin of these few moieties might be space filling probably connected with kinetics of demixing (homopolymer vs miktoatm star) and solidification. Owing to their diameter (∼60 nm) exceeding the periodicity of the lamellar structure, these globules or curved lamellae, shown in Figure 7, could be responsible for the systematic up-turn of the SAXS intensity (Figure 4) at low q's for blend A. Self-consistent field-theory calculations in ternary diblock copolymer/homopolymer blends identified a nonperiodic lamellar phase consisting of a random sequence of thin and thick domains.[19]

4. Conclusion

The possibility of controlling the phase separation in immiscible polymer blends via ionic interactions of the end groups has been explored in the past. It was shown that the electrostatic interactions between the end ions are able to overcome the thermodynamic repulsion of the polymeric backbones giving rise to the formation of diblock copolymers. In the present investigation, we have shown that the same interactions can be employed to form more complex block copolymer architectures. Mixing polystyrenes having three dimethylamine groups at one end with sulfonic acid terminated polyisoprenes in appropriate proportions results in the formation of $(PI)_n$-PS miktoarm star block copolymers. The formation of ionic pairs in the copolymers is strong, and the system remains in the microphase-separated state to very high temperatures.

References and Notes

(1) Horrion, J.; Jerome, R.; Teyssie, Ph. *J. Polym. Sci., Part C* **1986**, *24*, 69.
(2) Horrion, J.; Jerome, R.; Teyssie, Ph. *J. Polym. Sci., Part A* **1990**, *28*, 153.
(3) Russell, T. P.; Jerome, R.; Charlier, O.; Foucart, M. *Macromolecules* **1988**, *21*, 1709.
(4) Floudas, G.; Fytas, G.; Pispas, S.; Hadjichristidis, N.; Pakula, T.; Khokhlov, A. R. *Macromolecules* **1995**, *28*, 5109.
(5) Pispas, S.; Floudas, G.; Hadjichristidis, N. *Macromolecules* **1999**, *32*, 9074.
(6) Floudas, G.; Pispas, S.; Hadjichristidis, N.; Pakula, T. *Macromol. Chem. Phys.* **2001**, *202*, 1488.
(7) Hadjichristidis, N.; Iatrou, H.; Pispas, S.; Pitsikalis, M. *J. Polym. Sci., Part A: Polym. Chem.* **2000**, *38*, 3211.
(8) Tselikas, Y.; Iatrou, H.; Hadjichristidis, N.; Liang, K. S.; Mohanty, K.; Lohse, D. J. *J. Chem. Phys.* **1996**, *105*, 2456.
(9) Pispas, S.; Pitsikalis, M.; Hadjichristidis, N.; Dardani, P.; Morandi, F. *Polymer* **1995**, *36*, 3005.
(10) Quirk, R. P.; Kim, J. *Macromolecules* **1991**, *24*, 4515.
(11) Vanhoorne, P.; Grandjean, J.; Jerome, R. *Macromolecules* **1995**, *28*, 3553.
(12) Rosedale, J. H.; Bates, F. S. *Macromolecules* **1993**, *26*, 1740.
(13) Floudas, G.; Hadjichristidis, N.; Iatrou, H.; Pakula, T.; Fischer, E. W. *Macromolecules* **1994**, *27*, 7735.
(14) Rubinstein, M.; Obukhov, S. P. *Macromolecules* **1993**, *26*, 1740.
(15) Kawasaki, K.; Onuki, A. *Phys. Rev. A* **1990**, *42*, 366.
(16) Han, C. D.; Baek, D. M.; Kim, J. K.; Ogawa, T.; Sakamoto, N.; Hashimoto, T. *Macromolecules* **1995**, *28*, 5043.
(17) Milner, S. T. *Macromolecules* **1994**, *27*, 2333.
(18) Gerharz, B.; Du Chesne, A.; Lieser, G.; Fischer, E. W.; Cai, W. J. *J. Mater. Sci.* **1996**, *31*, 1053.
(19) Naughton, J. R.; Matsen, M. W. *Macromolecules* **2002**, *35*, 8926.

MA0256993